학술논문

한국터널공학회논문집 2009년 12월
제11권 제4호, pp. 427-435

An analytical solution for soil-lining interaction in a deep and circular tunnel

Seong-Won Lee[1]*, Jea-Hyeung Jeong[1], Chang-Yong Kim[1], Gyu-Jin Bae[1], Joo-Gong Lee[2], Kyung-Ho Park[3]

원형터널에서 지반-라이닝 상호작용에 대한 수학적 해석해에 관한 연구

이성원, 정재형, 김창용, 배규진, 이주공, 박경호

Abstract This study deals with the analytical solution for soil-lining interaction in a deep and circular tunnel. Simple closed-form analytical solutions for thrust and moment in the circular tunnel lining due to static and seismic loadings are developed by considering the relations between displacement and interaction forces at the soil-lining interface. The interaction effect at the soil-lining interface is considered with new ratios (the normal and shear stiffness ratios). The effects of the ratios on the normalized thrust and the normalized moment are investigated.

Keywords: Analytical solution, tunnel, tunnel lining, soil-lining interaction

요 지 본 연구는 원형 터널에서 지반-라이닝 상호작용에 대한 수학적 모델에 관한 연구를 다룬다. 정적, 동적 하중으로 인하여 터널 라이닝에서 발생하는 축력과 모멘트를 구하는 간단한 수학적 해가 제시되었다. 수학적 해를 유도하기 위하여 지반-라이닝의 경계면에서의 힘-변위 관계식을 고려하였고, 경계면에서의 상호작용을 고려하고자 새로운 계수비들을 제시하였다. 축력과 모멘트에 대한 계수비의 영향이 조사되었다.

주요어: 원형터널, 터널 라이닝, 지반-라이닝 상호작용, 이론적 해석

1. Introduction

Prediction of stress resultants (thrust and moment) in the lining due to static and seismic loadings is needed to evaluate the structural stability of the lining (Lee et al., 2008; Ha et al., 2008; Choi et al., 2009). Many efforts have been made to develop simple closed- form analytical solutions for the thrust and moment of tunnel linings due to static and seismic loadings in circular rock or soil tunnel (Burns and Richard, 1964; Höeg, 1968; Kuesel, 1969; Peck et al., 1972; Einstein and Schwartz, 1979; Wang, 1993; Penzien and Wu, 1998; Park et al., 2009). The existing analytical solutions are limited to the following assumptions: (1) full connection between soil and lining in the direction normal to the lining, (2) two extreme conditions (full-slip and no-slip conditions) in the tangential direction, (3) circular tunnel under plane strain condition, and (4) linear elastic behavior for soil and lining.

In any soil-structure interaction situation, relative movement of the structure with respect to the soil can occur. In numerical methods, interface or joint elements using the linear elastic and perfectly plastic constitutive model have been used to allow the differential movement of the soil and the structure at the soil-structure interface (Day and Potts, 1994).

This study deals with the analytical solutions for soil-lining interaction in a deep and circular tunnel. Simple closed-form analytical solutions for thrust and moment in the circular tunnel lining due to static and seismic loadings are developed by considering the relations

[1]Member, Korea Institute of Construction Technology
[2]BON E&C, Co., Ltd.,
[3]School of Engineering and Technology, Asian Institute of Technology
*교신저자: Seong-Won Lee (E-mail: swlee@kict.re.kr)

between displacements and interaction forces at the soil-lining interface. In order to consider the differential movement of the soil and the lining at the soil-lining interface, new normal and shear stiffness ratios, K_n and K_s, are introduced. The plane strain analysis assumes the linear elastic behavior for the media of the soil, the lining and the soil-lining interface element. The effects of the ratios on the normalized thrust and the normalized moment are investigated.

2. Definition of the problem

Consider a circular tunnel of radius R located sufficiently below the ground surface and subjected to horizontal and vertical accelerations from an earthquake loading as shown in Fig. 1. The stress state of the soil around the tunnel can be expressed as

$$\sigma_v = (1-k_v)\gamma H \tag{1}$$

$$\sigma_h = K(1-k_v)\gamma H \tag{2}$$

$$\tau = -k_h \gamma H \tag{3}$$

where σ_v and σ_h are the normal stresses, τ is the shear stress, k_v and k_h are the vertical and horizontal acceleration coefficients, K is the lateral earth pressure coefficient and γ is the unit weight of the soil over height H.

By neglecting the effect of vertical acceleration, the stress state of the soil around the tunnel during an earthquake can be considered by the sum of the static loading of σ_v and σ_h, and seismic loading of τ, as shown in Fig. 2. Further the stress state due to static loading can be divided into isotropic σ_i and deviatoric σ_d parts. The seismic loading is equivalent to a compressive and a tensile free-field principal stresses at 45° with the direction of the pure shear. It is required to solve for the thrust and moment in the lining due to static and additional seismic loadings.

The shear stress can also be estimated as(Penzien and Wu, 1998),

$$\tau = \frac{E_s \gamma_c}{2(1+\nu_s)} \tag{4}$$

where γ_c is the average free-field shear strain of the soil over the depth $2R$, which can be obtained from

$$\gamma_c = \frac{u(-R,t_c) - u(R,t_c)}{2R} \tag{5}$$

$u(y,t)$ is the horizontal free-field ground displacement with depth y and time t_c which produces the maximum shear-type deformation of the soil over the depth $2R$ of the intended tunnel, E_s is the Young's modulus of the soil, and ν_s is the Poisson's ratio of the soil.

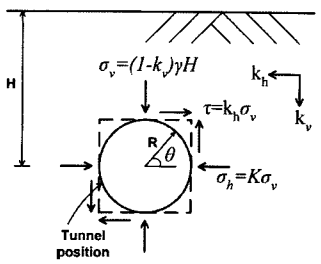

Fig. 1. A circular tunnel.

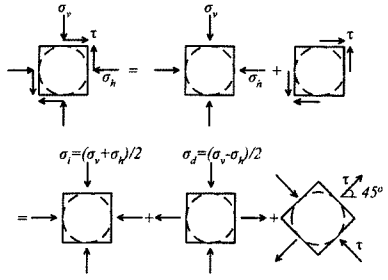

Fig. 2. State of stress during an earthquake.

3. Previous analytical solutions

The existing analytical solutions for thrust T_s and moment M_s due to static loading can be found for two extreme conditions (Einstein and Schwartz, 1979): for the full-slip condition at the soil-lining interface,

$$T_s = \frac{1}{2}(\sigma_v + \sigma_h)(1 + C_1)R + \frac{1}{2}(\sigma_v - \sigma_h)(1 - 2C_2)R\cos 2\theta \quad (6)$$

$$M_s = \frac{1}{2}(\sigma_v - \sigma_h)(1 - 2C_2)R^2 \cos 2\theta \quad (7)$$

where

$$C_1 = \frac{C^* F^* (1 - \nu_s)}{C^* + F^* + C^* F^* (1 - \nu_s)} \quad (8)$$

$$C_2 = \frac{(F^* + 6)(1 - \nu_s)}{2F^*(1 - \nu_s) + 6(5 - 6\nu_s)} \quad (9)$$

and for the no-slip condition at the soil-lining interface,

$$T_s = \frac{1}{2}(\sigma_v + \sigma_h)(1 + C_1)R + \frac{1}{2}(\sigma_v - \sigma_h)(1 + 2C_2)R\cos 2\theta \quad (10)$$

$$M_s = \frac{1}{4}(\sigma_v - \sigma_h)(1 - 2C_2 + 3C_3)R^2 \cos 2\theta \quad (11)$$

where

$$C_1 = \frac{C^* F^* (1 - \nu_s)}{C^* + F^* + C^* F^* (1 - \nu_s)} \quad (12)$$

$$\beta = \frac{(F^* + 6)C^*(1 - \nu_s) + 2F^* \nu_s}{3F^* + 3C^* + 2C^* F^* (1 - \nu_s)} \quad (13)$$

$$C_3 = \frac{C^*(1 - \nu_s)}{2\left[C^*(1 - \nu_s) + 4\nu_s - 6\beta - 3\beta C^*(1 - \nu_s)\right]} \quad (14)$$

$$C_2 = \beta C_3 \quad (15)$$

C^* and F^* are compressibility and flexibility ratios, which are measures of the extensional and flexural stiffness, respectively, defined as

$$C^* = \frac{E_s R(1 - \nu_l^2)}{E_l A_l (1 - \nu_s^2)} \quad (16)$$

$$F^* = \frac{E_s R^3 (1 - \nu_l^2)}{E_l I_l (1 - \nu_s^2)} \quad (17)$$

E_l, ν_l, I_l and A_l are the Young's modulus, the Poisson's ratio, the moment of inertia and the cross-sectional area of the lining, respectively.

4. Present analytical solutions

4.1 Static analysis

For convenience in analysis, the static loading condition in Fig. 2 will be separated into three cases: a circular cylindrical cavity subjected to excavation (Fig. 3(a)), a circular cylindrical lining subjected to contact stresses at the soil-lining interface (Fig. 3(b)), and a circular cylindrical cavity subjected to contact stresses at the soil-lining interface (Fig. 3(c)).

4.1.1 Interaction force and displacement distribution

(1) A cylindrical cavity subjected to excavation

If a circular tunnel is subjected to the static loading of σ_i and σ_d as shown in Fig. 3(a), the stresses around the cavity leads to the radial and circumferential displacement, u and v, respectively (Moore, 1994)

$$\begin{Bmatrix} u \\ v \end{Bmatrix} = \begin{Bmatrix} u_i + u_d \cos 2\theta \\ v_d \sin 2\theta \end{Bmatrix} \quad (18)$$

where

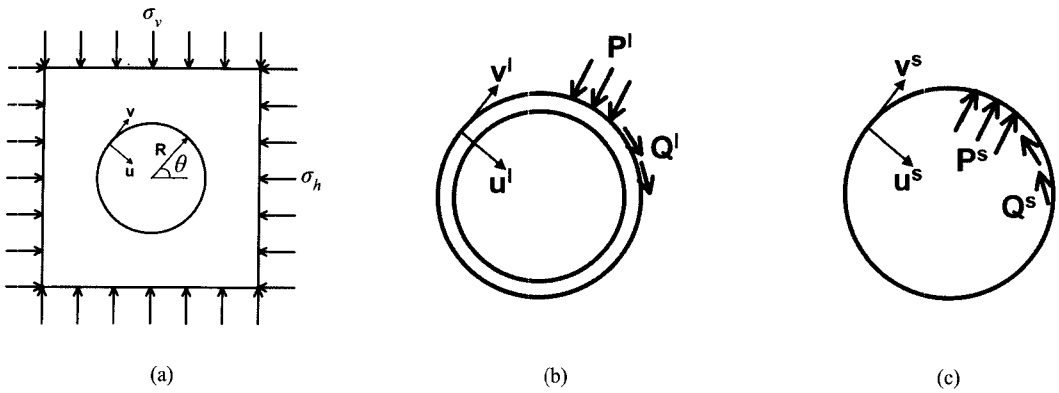

(a) (b) (c)

Fig. 3. Separation of static loading.

$$u_i = \frac{\sigma_i R}{2G_s} \tag{19}$$

$$\begin{Bmatrix} u_d \\ v_d \end{Bmatrix} = \frac{\sigma_d R(3-4\nu_s)}{2G_s} \begin{Bmatrix} 1 \\ -1 \end{Bmatrix} \tag{20}$$

$$\sigma_i = \frac{\sigma_v + \sigma_h}{2}, \quad \sigma_d = \frac{\sigma_v - \sigma_h}{2} \tag{21,22}$$

G_s is the shear modulus of the soil. Subscripts i and d indicate isotropic and deviatoric components, respectively.

If the lining is considered in the cavity, then the radial and circumferential forces per unit circumference, P and Q, develop across the soil-lining interface. The soil experiences the forces P^s and Q^s which lead to radial and circumferential displacements u^s and v^s, while the lining is subjected to forces P^l and Q^l leading to displacements u^l and v^l.

(2) A cylindrical lining subjected to contact stresses

The stress-displacement relations for the lining can be expressed as (Flügge, 1966; Einstein and Schwartz, 1979),

$$\frac{d^2v^L}{d\theta^2} + \frac{du^L}{d\theta} = -\frac{(1-\nu_l^2)R^2}{E_l A_l} Q^L \tag{23}$$

$$\frac{dv^L}{d\theta} + u^L + \frac{I_l}{A_l R^2}\left(\frac{d^4u^L}{d\theta^4} + 2\frac{d^2u^L}{d\theta^2} + u^L\right) = \frac{(1-\nu_l^2)R^2}{E_l A_l} P^L \tag{24}$$

From Eq. (18) and using the following equations,

$$u^L = u^l \cos 2\theta \tag{25a}$$

$$v^L = v^l \sin 2\theta \tag{25b}$$

$$P^L = P^l \cos 2\theta \tag{25c}$$

$$Q^L = Q^l \sin 2\theta \tag{25d}$$

the relationship between displacements u^l, v^l and interaction forces P^l, Q^l in the lining can be expressed using the influence matrix I^l,

$$u_i^l = I_i^l P_i^l \tag{26}$$

$$\begin{Bmatrix} u_d^l \\ v_d^l \end{Bmatrix} = I_d^l \begin{Bmatrix} P_d^l \\ Q_d^l \end{Bmatrix} \tag{27}$$

where

$$I_i^l = \frac{R^2(1-\nu_l^2)}{E_l A_l} \tag{28}$$

$$I_d^l = \begin{bmatrix} \frac{R^4(1-\nu_l^2)}{9E_lI_l} & -\frac{R^4(1-\nu_l^2)}{18E_lI_l} \\ -\frac{R^4(1-\nu_l^2)}{18E_lI_l} & \frac{R^4(1-\nu_l^2)}{36E_lI_l} + \frac{R^2(1-\nu_l^2)}{4E_lA_l} \end{bmatrix} \quad (29)$$

(3) A cylindrical cavity subjected to contact stresses

The response of a cylindrical cavity to a continuous cylindrical lining load can be obtained using the plane strain flexibility matrix I^s, (Moore, 1994)

$$u_i^s = I_i^s P_i^s \quad (30)$$

$$\begin{Bmatrix} u_d^s \\ v_d^s \end{Bmatrix} = I_d^s \begin{Bmatrix} P_d^s \\ Q_d^s \end{Bmatrix} \quad (31)$$

where

$$I_i^s = \frac{R}{2G_s} \quad (32)$$

$$I_d^s = \frac{R}{G_s} \begin{bmatrix} \frac{5-6\nu_s}{6} & -\frac{2-3\nu_s}{3} \\ -\frac{2-3\nu_s}{3} & \frac{5-6\nu_s}{6} \end{bmatrix} \quad (33)$$

4.1.2 Soil-lining interaction

In numerical methods, interface elements have been used to allow the differential movement of the soil and the structure at the soil-structure interface (Day and Potts, 1994). In this study, elastic normal and shear stiffnesses, k_n and k_s, are used to simulate the differential movement at the soil-lining interface. Then, using the flexibility equations for soil and lining and introducing normal and shear stiffness ratios, K_n and K_s, the interaction forces can be evaluated for interface condition.

(a) Uniform response

For the uniform response of the soil-lining system, the following equilibrium of interaction forces and compatibility of displacements can be considered:

$$P_i^s + P_i^l = 0 \quad (34)$$

$$u_i = u_i^l - u_i^s + \frac{1}{k_n} P_i^l \quad (35)$$

By substituting the appropriate equations in (18)~(33) into (34)~(35), one can obtain

$$P_i^l = \frac{1}{\left\{\frac{R^2(1-\nu_l^2)}{E_lA_l} + \frac{R}{2G_s} + \frac{1}{k_n}\right\}} \frac{\sigma_i R}{2G_s} \quad (36)$$

Using the compressibility ratio C and the normal stiffness ratio K_n, defined as

$$C = \frac{E_s(1-\nu_l^2)R}{E_lA_l(1+\nu_s)(1-2\nu_s)} \quad (37)$$

$$K_n = \frac{E_s}{2(1+\nu_s)(1-2\nu_s)Rk_n} \quad (38)$$

Eq. (36) can be rewritten as

$$P_i^l = \frac{1}{\{(C+2K_n)(1-2\nu_s)+1\}} \sigma_i \quad (39)$$

(b) Deviatoric response

Consider the following equilibrium of interaction forces and compatibility of displacement for the deviatoric response of the soil-lining system,

$$P_d^s + P_d^l = 0 \quad (40)$$

$$Q_d^s + Q_d^l = 0 \quad (41)$$

$$\begin{Bmatrix} u_d \\ v_d \end{Bmatrix} = \begin{Bmatrix} u_d^l \\ v_d^l \end{Bmatrix} - \begin{Bmatrix} u_d^s \\ v_d^s \end{Bmatrix} + \begin{bmatrix} \frac{1}{k_n} & 0 \\ 0 & \frac{1}{k_s} \end{bmatrix} \begin{Bmatrix} P_d^l \\ Q_d^l \end{Bmatrix} \quad (42)$$

When $k_n \to \infty$ and $k_s \to \infty$, Eqs. (40)~(42) represent the no-slip interface condition. When $k_n \to \infty$ and $k_s \to 0$, Q_d^s and Q_d^l vanish, which means the lining is subjected to sliding along the interface.

By substituting the appropriate equations in (18)~(33) into (40)~(42), one can obtain

$$\begin{Bmatrix} P_d^l \\ Q_d^l \end{Bmatrix} = \frac{\sigma_d R(3-4\nu_s)}{2G_s\Delta} \begin{Bmatrix} \frac{R^2(1-\nu_l^2)}{4E_lA_l} - \frac{R^4(1-\nu_l^2)}{36E_lI_l} + \frac{R}{6G_s} + \frac{1}{k_s} \\ -\frac{R^4(1-\nu_l^2)}{18E_lI_l} - \frac{R}{6G_s} - \frac{1}{k_n} \end{Bmatrix} \quad (43)$$

where

$$\begin{aligned} \Delta = & \frac{R^2(1-\nu_l^2)}{4E_lA_l}\left\{\frac{R^4(1-\nu_l^2)}{9E_lI_l} + \frac{R(5-6\nu_s)}{6G_s}\right\} + \frac{R^5(1-\nu_l^2)(3-2\nu_s)}{72E_lI_lG_s} \\ & + \left\{\frac{R(3-4\nu_s)}{12G_s}\right\}^2 + \frac{1}{k_n}\left\{\frac{R^4(1-\nu_l^2)}{36E_lI_l} + \frac{R^2(1-\nu_l^2)}{4E_lA_l} + \frac{R(5-6\nu_s)}{6G_s}\right\} \\ & + \frac{1}{k_s}\left\{\frac{R^4(1-\nu_l^2)}{9E_lI_l} + \frac{R(5-6\nu_s)}{6G_s}\right\} + \frac{1}{k_nk_s} \end{aligned} \quad (44)$$

Using the flexibility ratio F and the shear stiffness ratio K_s, defined as

$$F = \frac{E_s(1-\nu_l^2)R^3}{6E_lI_l(1+\nu_s)} \quad (45)$$

$$K_s = \frac{E_s}{2(1+\nu_s)Rk_s} \quad (46)$$

Eqs. (43) and (44) can be rewritten as

$$\begin{Bmatrix} P_d^l \\ Q_d^l \end{Bmatrix} = \frac{\sigma_d(3-4\nu_s)}{\Delta'} \begin{Bmatrix} -F + 1.5(1-2\nu_s)C + 2 + 12K_s \\ -2(F+1) - 12(1-2\nu_s)K_n \end{Bmatrix} \quad (47)$$

where

$$\begin{aligned} \Delta' = & \{(3-2\nu_s) + (1-2\nu_s)C\}F + (2.5 - 8\nu_s + 6\nu_s^2)C + 6 - 8\nu_s \\ & + K_n(1-2\nu_s)\{2F + 3(1-2\nu_s)C + 4(5-6\nu_s)\} \\ & + 4K_s\{2F + 5 - 6\nu_s\} + 24(1-2\nu_s)K_nK_s \end{aligned} \quad (48)$$

Note that when K_n=K_s=0, Eqs. (47) and (48) represent the no-slip interface condition, whereas the case of K_n=0 and $K_s \to \infty$ indicates the full-slip interface condition.

Then, the thrust and the moment in the lining due to static loading of σ_i and σ_d can be obtained:

$$T_s = T_i + T_d\cos 2\theta \quad (49)$$

$$M_s = M_d\cos 2\theta \quad (50)$$

where

$$T_i = P_i^l R \quad (51)$$

$$T_d = \frac{R}{3}\left(-P_d^l + 2Q_d^l\right) \quad (52)$$

$$M_d = \frac{R^2}{3}\left(-P_d^l + \frac{Q_d^l}{2}\right) \quad (53)$$

4.2 Seismic analysis

As mentioned in Section 2, the shear stress due to additional seismic loading is equivalent to a compressive and a tensile free-field principal stresses at 45° with the direction of the pure shear. So the thrust and moment due to additional seismic loading can be obtained by simply substituting τ for σ_d and $cos2(\theta+\pi/4)$ for $cos2\theta$ in Eqs. (49)~(53). However, since the shear stress is generated after the cavity is opened, the following σ_d is considered:

$$\sigma_d = \frac{2(1-\nu_s)}{(3-4\nu_s)}(\sigma_v - \sigma_h) = \frac{4(1-\nu_s)}{(3-4\nu_s)}\tau \quad (54)$$

Therefore, the thrust and the moment due to additional seismic loading can be obtained:

$$T_e = T_d\cos 2\left(\theta + \frac{\pi}{4}\right) \quad (55)$$

$$M_e = M_d\cos 2\left(\theta + \frac{\pi}{4}\right) \quad (56)$$

where subscript e indicates the solution for additional seismic loading.

5. Definition of stiffness ratios for interface element

In the previous researches (Burns and Richard, 1964; Höeg, 1968; Peck et al., 1972), the relative stiffness of the lining and the soil is characterized by two ratios (the compressibility ratio and the flexibility ratio). The compressibility ratio C is a measure of the extensional stiffness of the soil relative to that of the lining, while the flexibility ratio F is a measure of the flexural stiffness of the soil relative to that of the lining: (Peck et al., 1972)

$$C=\frac{\left(\frac{P}{\Delta D/D}\right)_{soil}}{\left(\frac{P}{\Delta D/D}\right)_{lining}}=\frac{E_s}{(1+\nu_s)(1-2\nu_s)}\cdot\frac{R(1-\nu_l^2)}{E_lA_l} \tag{57}$$

$$F=\frac{\left(\frac{P}{\Delta D/D}\right)_{soil}}{\left(\frac{P}{\Delta D/D}\right)_{lining}}=\frac{E_s}{(1+\nu_s)}\cdot\frac{R^3(1-\nu_l^2)}{6E_lI_l} \tag{58}$$

In a similar way, the normal stiffness ratio and the shear stiffness ratio are introduced to characterize the relative stiffness of the soil and the interface element. The normal stiffness ratio K_n is obtained for a uniform external pressure,

$$K_n=\frac{\left(\frac{P}{\Delta D/D}\right)_{soil}}{\left(\frac{P}{\Delta D/D}\right)_{interface}}=\frac{E_s}{(1+\nu_s)(1-2\nu_s)}\cdot\frac{1}{2Rk_n} \tag{59}$$

and the shear stiffness ratio K_s is obtained for a pure shear,

$$K_s=\frac{\left(\frac{P}{\Delta D/D}\right)_{soil}}{\left(\frac{P}{\Delta D/D}\right)_{interface}}=\frac{E_s}{(1+\nu_s)}\cdot\frac{1}{2Rk_s} \tag{60}$$

6. Effects of normal and shear stiffness ratios

The interaction effect at the soil-lining interface is included using the normal and shear stiffness ratios. The effects of these ratios on the normalized thrust and the normalized moment are investigated using the values of ν_s=0.35, ν_l=0.15, C=1.0, F=1.0.

Figs. 4 and 5 show the results of normalized thrust and moment distributions with respect to K_s for K =0.5 and K_n=0, while the results for K=2.0 are shown

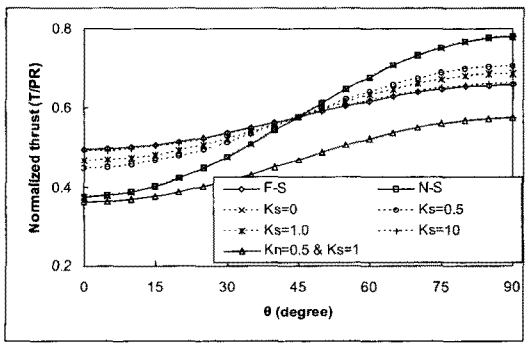

Fig. 4. Normalized thrust (K=0.5, K_n=0).

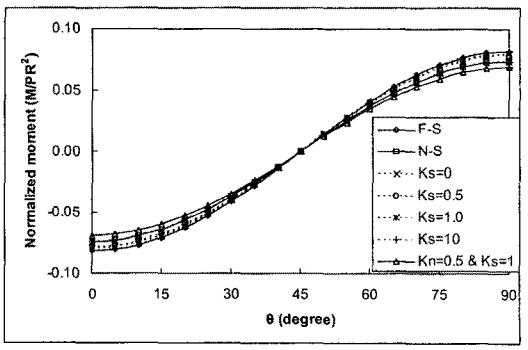

Fig. 5. Normalized moment (K=0.5, K_n=0).

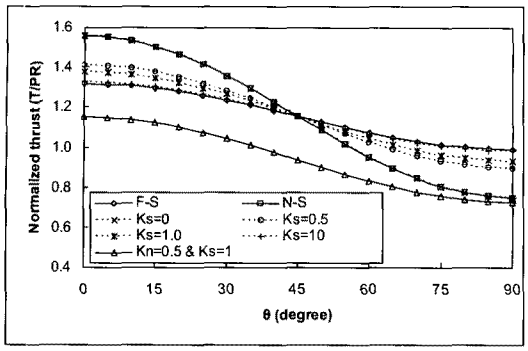

Fig. 6. Normalized thrust (K=2.0, K_n=0).

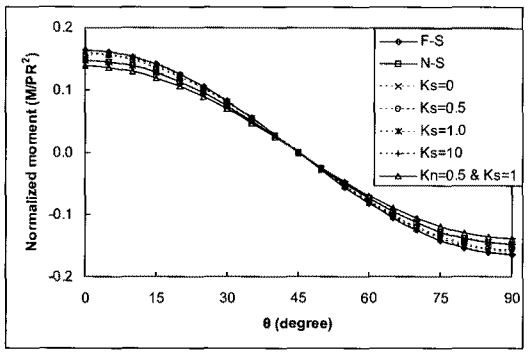

Fig. 7. Normalized moment (K=2.0, K_n=0).

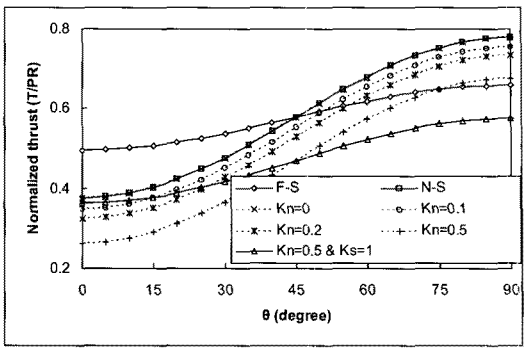

Fig. 8. Normalized thrust (K=0.5, K_s=0).

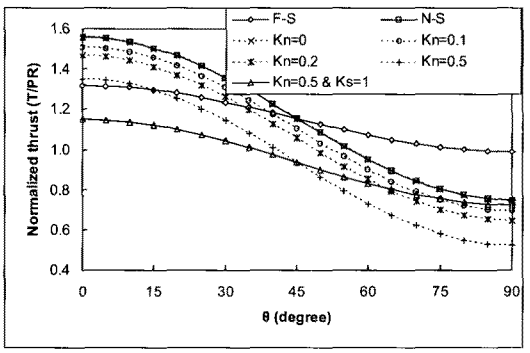

Fig. 9. Normalized thrust (K=2.0, K_s=0).

in Figs. 6 and 7. For comparison, the results for full-slip (F-S) and no-slip (N-S) conditions, and the case of K_n=0.5 and K_s=1 are also shown in the figures. θ=90° indicates the tunnel crown, while θ=0 indicates the tunnel springline. As expected, the case of K_n=K_s=0 gives the same results as those of no-slip interface condition. The normalized thrust increases with the decrease of K_s from the full-slip condition to the no-slip condition. The normalized moment decreases as K_s decreases from the full-slip condition to the no-slip condition. While the shear stiffness ratio K_s can theoretically vary from zero to infinity, Figs. 4 to 7 show that the shear stiffness ratio seems to be limited to a certain range.

Figs. 8 and 9 show the results of normalized thrust with respect to K_n for K=0.5 and 2.0 respectively, with K_s=0. The normalized thrust increases with the decrease of K_n. The normalized moment decreases as K_n increases.

7. Conclusions

Simple closed-form analytical solutions for thrust and moment in the lining of a deep and circular tunnel due to static and seismic loadings have been presented by considering the relations between displacements and interaction forces at the soil-lining interface. The normal stiffness ratio and the shear stiffness ratio are introduced as a means of defining interface element stiffness. Unlike the existing analytical solutions, which consider only two extreme conditions (the full-slip

interface condition and the no-slip interface condition), new solutions allow the differential movement of the soil and the lining at the soil-lining interface.

The no-slip interface condition is one extreme case of K_n=K_s=0, whereas the full-slip interface condition is the other extreme case of K_n=0 and $K_s \rightarrow \infty$. The normalized thrust increases with the decrease of K_n and K_s. The normalized moment decreases with the decrease of K_s and the increase of K_n.

References

1. Burns, J.Q. and Richard, R.M. (1964), Attenuation of stresses for buried cylinders. In Proceedings of the Symposium on Soil-Structure Interaction, University of Arizona, AZ, pp. 378-392.
2. Choi, S.H., Park, I.J. and Kim, S.H. 2009. Aseismic analysis for large underground structure. Tunnelling Technology, 11(2), pp. 163-174.
3. Day, R.A. and Potts, D.M. 1994. Zero thickness interface elements-numerical stability and application. International Journal for Numerical and Analytical Methods in Geomechanics, 18, pp. 689-708.
4. Einstein, H.H. and Schwartz, C.W. 1979. Simplified analysis for tunnel supports. Journal of the Geotechnical Engineering Division, 105, pp. 499-518.
5. Flügge, W. 1966. Stresses in shells, Springer-Verlag, Inc., New York, N.Y.
6. Ha, T.W., Kim, D.Y., Shin, Y.W. and Yang, H.S. 2008. Evaluation methods of shotcrete lining stresses considering steel rib capacities by two-dimensional numerical analysis. Tunnelling Technology, 10(3), pp. 269-282.
7. Höeg, K. 1968. Stresses against underground structural cylinders. Journal of the Soil Mechanics and Foundations Division, 94, pp. 833-858.
8. Kuesel, T.R. 1969. Earthquake design criteria for subways. Journal of the Structural Engineering Division, 95(6), 1213-1231.
9. Lee, G.P., Lee, S.W., Shin, H.S. and Hwang, J.H. 2008. Mechanical behavior of tunnel liner using precast segment reinforced by rib. Tunnelling Technology, 10(3), 295-302.
10. Moore, I.D. 1994. Analysis of rib supports for circular tunnels in elastic ground. Rock Mechanics and Rock Engineering, 27, pp. 155-172.
11. Park, K.H., Tantayopin, K., Tontavanich, B. and Owatsiriwong, A. 2009. Analytical solution for seismic-induced ovaling of circular tunnel lining under no-slip interface conditions: a revisit. Tunneling and Underground Space Technology, 24, pp. 231-235.
12. Peck, R.B., Hendron, A.J. and Mohraz, B. 1972. State of the art in soft ground tunneling. In Proceedings of the First Rapid Excavation and Tunneling Conference, American Institute of Mining, Metallurgical, and Petroleum Engineers, NY, pp. 259-286.
13. Penzien, J. and Wu, C.L. 1998. Stresses in linings of bored tunnels. Earthquake Engineering and Structural Dynamics, 27, pp. 283-300.
14. Wang, J.N. 1993. Seismic design of tunnels. Parsons Brinckerhoff Quade & Douglas, Inc., NY, Monograph 7.

접수일(2009.9.10), 수정일(2009.10.15), 게재확정일(2009.10.19)